

AN ORIGINAL NEUTRON GENERATOR USING A SHORT STRUCTURE ACCELERATING SYSTEM AND TURBOMOLECULAR PUMPING

C.Fremiot and J.Muel
Centre d'Etudes Nucléaires
Grenoble France

1 Introduction

Experience has shown that commercially available electrostatic accelerators are unsuited, generally, for the generation of monoenergetic neutron flux on the basis of the d, t , reaction.

The following major disadvantages are usually encountered in this particular function :

- limited ion currents at the target
- too much beam regulation (intensity, energy, form), which complicates maintenance.

Thus, the authors decided to undertake the design of an accelerator for this purpose only, and possessing the following characteristics :

- fixed acceleration voltage : 240 kV
- fixed beam diameter at target : 3 cm
- fixed peak beam intensity : 10 mA.
- dutyratio : 1/100
- pulse length : variable from 100 μ s to 10 ms.

The components of a "standard" accelerator were first modified or redesigned to obtain :

- an ion source capable of the required beam intensity
- a modulated radiofrequency oscillator
- a single gap accelerator tube
- a stable acceleration voltage
- a reliable and efficient vacuum system

and a first model was then built and equipped with these components. For reasons of bulk, we were obliged to limit acceleration voltage to 130 kV. Satisfactory results having been obtained with this experimental assembly, we undertook the production of a full scale unit.

2 Description of Components

2.1 - Ion source

The high frequency linear discharge source designed in our laboratory¹ is intended to supply 3 mA d.c. ion beams. It can reach 5 mA, but at this limit, the ratio of extraction current to out put ion current rises steeply, which seems to indicate that part of the beam is intercepted by the extraction canal. To get around this difficulty, which we attribute to the space charge, we increased the diameter of the canal as shown in figure 1.

This modification made it possible to extract ion currents of 12 mA peak, maximum performance being situated around 14 mA

duty ratio of 1/100.

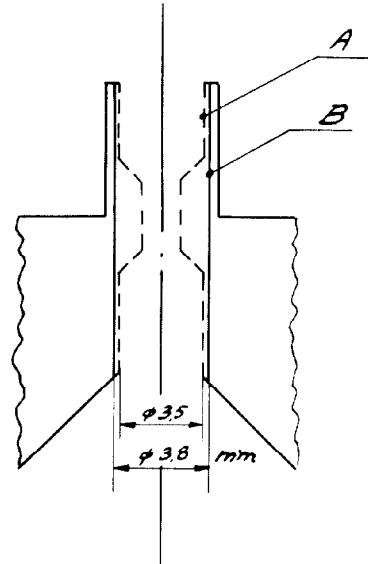


Fig.1 Old (A) and actual (B) size of the extraction canal.

As the peak ion current is fixed at 10 mA, the mean current is 100 μ A, which explains the small difference between the gaseous flow rates in pulsed operation and those required for 3 mA d.c.

In view of the low power levels involved, we did not consider it necessary to pulse the extraction current, which is thus continuously applied. We observed that the orientation of the lines of force of the protective radial magnetic field was a critical parameter : a deviation of as little as $\pm 5^\circ$ from the preferential direction totally destroyed the stability of source operation.

The Hartley-type oscillator is capacitor-coupled to the source.

The modulator supplies adjustable-width voltage pulses which are applied to the cathode of the oscillator tube across a suitably dimensioned pulse transformer.

The peak RF power required is about 600 W, and oscillation frequency is regulated to about 60 Mc/s.

The beam extraction voltage is supplied by a full wave voltage doubler system.

The axial magnetic field is also permanently applied.

All the above equipment is supplied power at 127 V - 50 c/s by a voltage-regu-

brought to the accelerator voltage potential, and its drive motor is connected to ground. The drive shaft is insulated.

2.2. - Acceleration voltage

This voltage is obtained from a Sames 300 kV - 1.5 mA electrostatic generator piloted by a standard "Average Stability" system limiting HV variations to $\pm 1\%$. In pulsed operation and under the experimental conditions involved, calculation indicated that a storage capacitance of about 200 pF had to be associated with the machine; this is less than the stray capacitance inherent to this type of generator, and therefore favours choice of this type of voltage supply.

We checked HV stability in the pulsed mode as follows: a diaphragm was placed in front of the target, both being mobile along the axis of the beam. The greater the distance from the electrode orifice, the less the diaphragm current; a point can be determined at which it becomes nil. At this point, 10 kV change in acceleration voltage results in the appearance of 1 mA current at the diaphragm, and a corresponding decrease in target current.

As the function $I_{\text{diaph.}} = f(V_{\text{acc}})$ is practically linear for small V_{acc} variations, it can be assumed that a change of 1 kV of V_{acc} will produce a change of 0.1 mA in $I_{\text{diaph.}}$, an amplitude that can be easily detected on the screen of an oscilloscope visualizing diaphragm current.

Stability for 100 kV being ± 1 kV, we checked this assumption at positions close to the point of current appearance at the diaphragm. During these checks, we observed that acceleration voltage was not affected by any interference or disturbance, thereby confirming the efficiency of a device employing a storage capacitance, and our estimation of stray capacitance.

2.3. - Vacuum System

A high degree of availability is demanded of the accelerator³. The performances required of the vacuum system are thus:

- a sustained vacuum of 1 to a few 10^{-6} Torr, which is the best range for efficient operation
- indefinite, continuous operation, and in the event of halts due to power outages, automatic re-starting
- re-establishment of the specified vacuum, after exposure to the atmosphere, within a minimum period
- absence of pollution, particularly of the targets in the accelerator.

The makers of pump seem to consider that the diffusion pump meets all the above requirements satisfactorily. However, we find that it has several drawbacks:

- high liquid nitrogen consumption: 200 litres par week by a mercury vapour pump of 600 litres par sec. represent an annual expenditure of 10,000 French Francs

(or 2,000 Dollars).

- lack of reliability in unsupervised operation during week-ends, etc.
- clumsiness of automatic restarting after power outages
- extra down-times for periodic heating and cleaning of the trap
- risk of pollution by mercury in the event of automatic trap feed failure.

To obviate these disadvantages, while maintaining flexibility, we opted for a set employing a turbomolecular pump.

In the case considered, it is a question of evacuating the deuterium gas leaving the ion source, a flow of about 10 cubic centimeters per hour, T.P.N., or about 2×10^{-3} l.t.s.⁻¹

We determined that for efficient accelerator operation, the internal pressure must be better than 10^{-5} Torr, which must therefore be maintained by a vacuum system capable of a flowrate for deuterium of more than $\frac{2 \times 10^{-3}}{10^{-5}} = 200$ litres par sec.

But another problem arose. The compression ratio of turbopumps is not high for light gas. The compression ratio, would be a few 10^3 for deuterium, according to the makers, and would be still lower with the pump operative. Thus to maintain a vacuum of a few 10^{-6} Torr, a primary pressure of less than 10^{-3} Torr would have to be ensured, which for the source corresponds to a primary delivery at this pressure of about 10 m³ per hour.

In view of the above, we finally chose to employ a set comprised of a 250 litres par sec. turbopump and a primary pump rated for 10 m³ per hour (TVP 900/R 010).

We determined experimentally on the operative set that the pumping rate for deuterium is substantially better than nominal. The system includes a variable conductance (C) nozzle (fig.2)

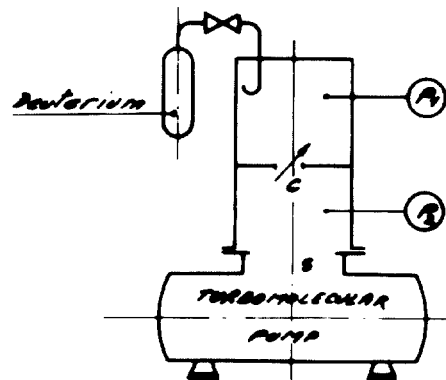


Fig. 2.

pressures are measured and the pumping rate S and gas-flow Q (or deuterium flowrate) are deduced by equating : $P_1 = \frac{1}{S} + \frac{1}{C}$

or for greater rigour, P_1 is plotted = $f(\frac{1}{C})$ by measuring P_1 for various C values, whereby the abscissa at origin gives us $\frac{1}{S}$ and the slope gives us Q (fig. 3). This is done for several values of Q.

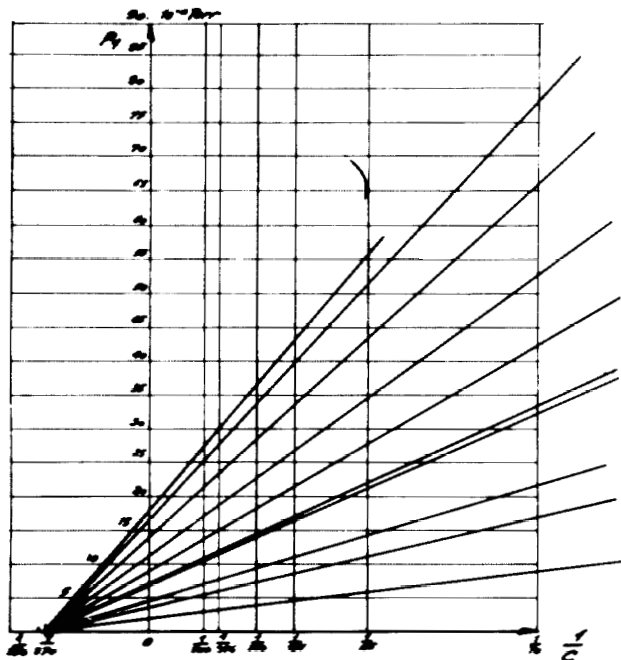


Fig. 3.

The turbomolecular pump is directly connected to the accelerator, without intervening cold trap or valve, and primary vacuum tubing has been reduced to the strict minimum necessary. The following, in the order stated, are situated between the primary and secondary pumps : a Pirani gauge, a pneumatically actuated valve under the control of the Pirani gauge readings.

There is neither a by-pass nor a primary trap : the high compression ratio of the turbopump for heavy molecules makes it an efficient barrier to pollution of the enclosure by oil from the primary pump (and the pneumatic valve closes automatically if the primary pump ceases to operate). Rapid partial pressure analysis with a VEECO analyser showed that H_2O was principally present, with residual H_2 towards the end. No traces of hydrocarbides could be detected (fig.4)

The system includes an automatic nitrogen injector controlled by a timer and injecting nitrogen at 10 Torr in the event of pauses in operation of more than 20 minutes : this blocks the slow migration

of oil from the bearings of the primary pump towards the accelerator tube.

From the operational standpoint, the normal condition of the set is when it is "continuously operative". There are three transient conditions :

- startup with the enclosure at atmospheric pressure. Pre-exhaustion is through the turbomolecular pump, which starts a few minutes later, when the gauge J_1 indicates less than 4×10^{-2} (fig.5)

- startup with the enclosure exhausted, after power outages : this is automatic, as soon as power reappears, and is as indicated above.

- re-exhaustion of the target chamber the chamber is exhausted to a few 10^{-2} approx. by an auxiliary pump and connected to the vacuum system without any particular precautions.

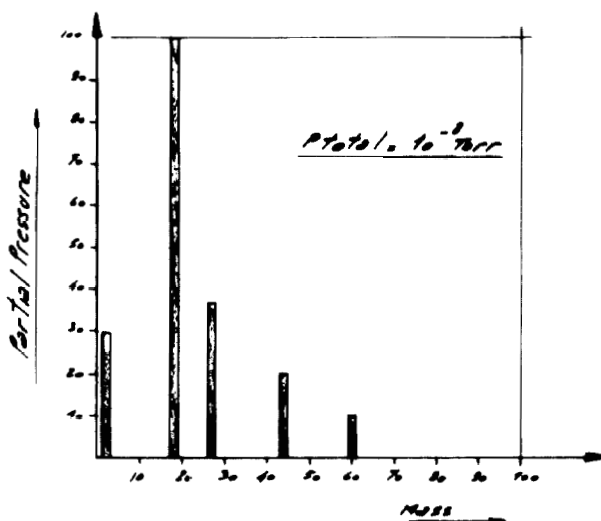


Fig. 4.

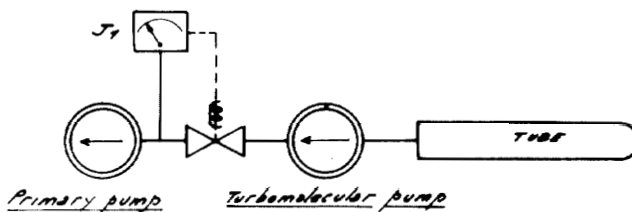


Fig. 5.

2.4. - Experimental Rig

Figure 8 is a schematic of the experimental rig produced. The acceleration voltage is applied between plates C and G, the latter connected to ground potential. Electrode J can be shifted along the focus axis to vary the source-electrode hole distance. The electrode is isolated from ground by the araldite ring F to permit reading of its bombardment.

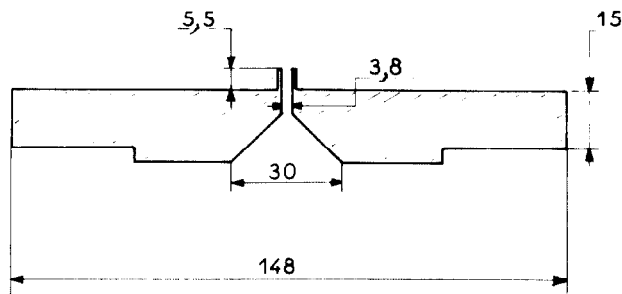


Fig. 6.

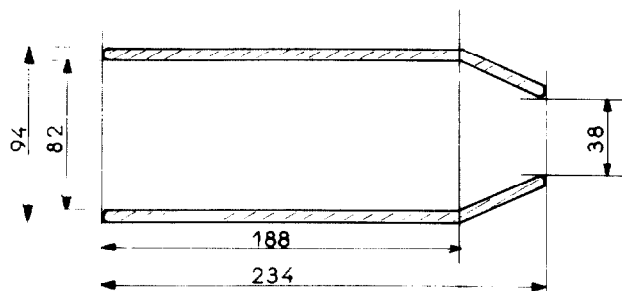


Fig. 7.

- Figures 6 and 7 show the size of the source mounting and acceleration electrode.

For study of beam geometry, we produced a simple system which afforded excellent results :

- the electrons trap, diaphragme, and target constitute a rigid assembly joined by insulating supports. The assembly is connected to a rod V sliding in an impervious SEAVOM type JWT 1970 passthrough. These measuring facilities are centered in motion by three nylon rollers bearing on the inner surface of the electrode.

- rod V is driven by a motor under remote control from the console. Repetition of target position at the console was not considered necessary, although this could have been obtained by coupling a helipot to the drive motor shaft.

- each electrical measurement point (electrode, target, etc.) is grounded across a 1000Ω resistor which can be rapidly switched to the oscilloscope with T. The resistance value of $1 \text{ k}\Omega$ was chosen because it permits direct readings in mA on the oscilloscope screen, graduated in volts, and because sufficiently low not to involve difficulties due to interference fields liable to induce stray voltages in connection cables.

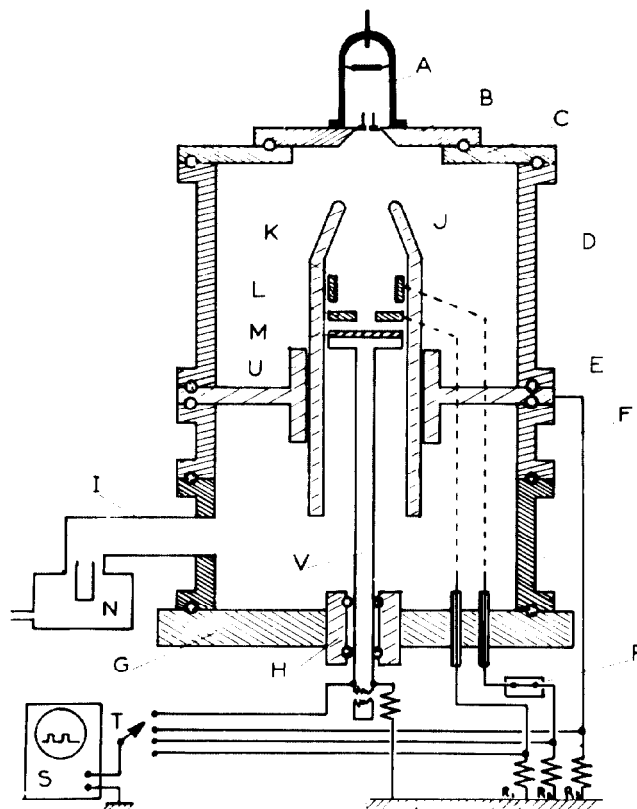


Fig. 8.

Fig. 8 - A Discharge vessel. B Source mounting. C Superior plate. D Superior ring. E Electrode holding plate. F Araldite ring. G Low plate. H Sliding passthrough. I Pumping junction. J Electrode. K electron trap. L Diaphragme. M Target. N pumping system. P Trap voltage supply. R1, R2, R3 $1 \text{ k}\Omega$ resistors. S Oscilloscope. T Four points switch. V Sliding rod.

3 Results obtained with the model

For our geometry and experimental conditions, we first determined the maximum voltages permissible between electrode and source, as a function of the distance between them.

For this, we produced an accessory rig, in which a metal model of the source plate can be positioned at a distance d from a fixed plate. The voltages U_k between these electrodes was then measured for various d values and for ; no leakage current I_f , for $I_f = 50 \mu\text{A}$, and for dielectric breakdown (flashover).

The three values were determined at various pressures, adjusted by varying a flow of injected hydrogen.

The test determined that a field of 50 kV/cm could be tolerated in all safety, and a field of 100 kV/cm with some precautions. The following are indicative of the Uk values measured :

d=5 mm p=30x10⁻⁶ Torr Uk=49 kV If=0
 d=5 mm p=30x10⁻⁶ Torr Uk=60 kV If=50 µA
 d=5 mm p=30x10⁻⁶ Torr Uk=100 kV flashover

We then went over to the experimental rig shown in figure 8 and measured the following general values :

	Vacc 130 kV	Vacc 90 kV
I diaph	0,3 mA	1 mA
I electrode	0,3 mA	0
I target	9 mA	8 mA

For :

- beam diameter 3 cm
- source-elct. gap 5 cm
- target-elct. hole gap . :10 cm
- elect. hole diameter .. 4.5 cm

It is to be noted that beam intensity was maintained at 9 mA peak owing to modulator failure.

We also determined the position of the diaphragme-trap-target assembly for 8 mA peak target current, 1 mA diaphragme current, and various acceleration voltages

Vacc (kV)	Movement along axis (cm)
50	0
60	1
70	2.5
80	4
90	6
100	8

In conclusion, the above results tend to indicate that acceleration voltages of more than 130 kV can be employed : at 240 kV, beam concentration will be greater, that is to say that to reobtain a 3 cm beam diameter at the target, one of three steps may be taken :

- increasing the electrode-source gap
- increasing the electrode aperture diameter
- increasing the elect. aperture to target gap

It is clear that any of the three - which can also be combined - is compatible with good performance versus voltage of the accelerator components, despite increasing acceleration voltage.

4 Final Model.

Our twofold intention was to produce a facility for routine irradiations and at the same time a prototype capable of modification as dictated by experience.

The final model may be considered in four parts :

- the acceleration system
- the source power supply
- the HV generator

and instrumentation providing readings of the : - currents and voltages (target, diaphragme, etc.)

- pressure in the tube

The techniques employed being quite conventional, a more detailed description seems superfluous.

4.2 - Accelerator (see fig. 9)

The accelerator tube and acceleration system are mounted in a steel pipe cradle 13 equipped with castors and jacks.

The tube consists of a stack of porcelain sections 1,2,3,4 welded to interposed plates carrying the equipotential rings 8. The rings are linked by resistors distributing the overall acceleration voltage.

The upper tube closure is in the form of a steel tank 9 with an opening to be covered by the source slab.

The lower closure is a nickel-steel plate 6 with two openings, one for the beam, the other for the vacuum system.

The hood 12 protects the walls of the tube against rising metal particles.

The target, secondary electron trap, and diaphragme are not shown in the drawing ; their positions will be experimentally determined under the base plate.

4.3 - HV generator

We intend to provide a SAMES 300 kV - 7 mA, equipped with a mean stability regulator. The performances of this machine are more than required at present, but our project includes raising the ion beam to 50 mA peak.

4.4. - Source power supply (fig.10)

This will group all source power facilities, the primary power source alternator 8, and the variacs regulating currents and voltages within an enclosure at acceleration voltage potential. The enclosure is supported by a "HAEFFELY" tube 6 mounted on a frame housing the alternator drive 9 and variac drives. All transmission shafts are insulating.7.

An opening is provided at the top for televised (closed loop) viewing of the instruments mounted on the power chassis. Connecting conductors between this assembly and the source are contained in a metal conduit.

References

- 1 C.FREMIOT Rapport CEA N° 2266 - 1963
- 2 N.FELICI Electrostatique et Electronique Onde Electrique tome XXXVII
- 3 R.GERBIER J.MUEL Emploi d'une turbopompe sur un accélérateur électrostatique Le Vide N° 124 pp 283-286

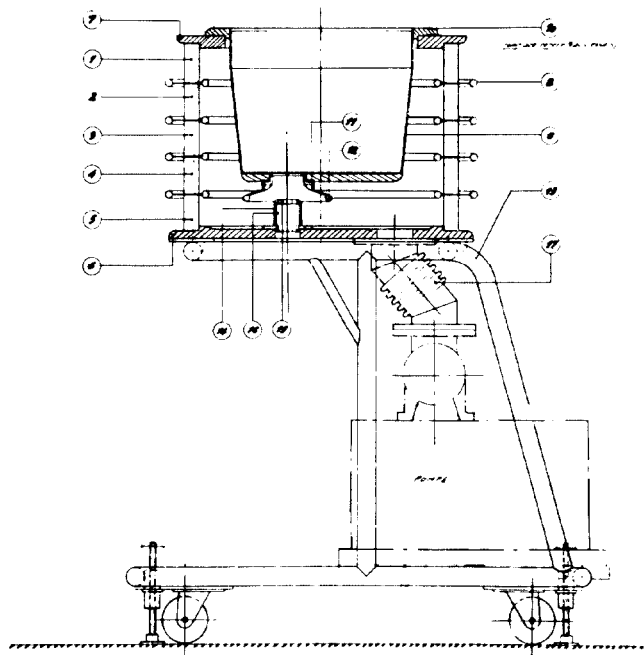


Fig. 9.

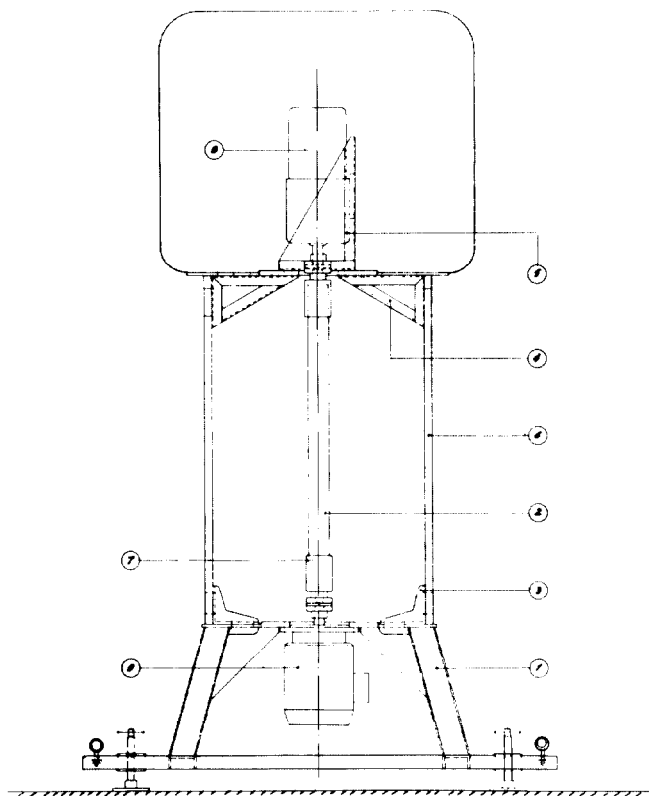


Fig. 10.